ADVANCED MATERIALS
www.advmat.de

Tunable Electroluminescence in Planar Graphene/SiO_2 Memristors

*Congli He, Jiafang Li, Xing Wu, Peng Chen, Jing Zhao, Kuibo Yin, Meng Cheng, Wei Yang, Guibai Xie, Duoming Wang, Donghua Liu, Rong Yang, Dongxia Shi, Zhiyuan Li, Litao Sun, and Guangyu Zhang**

Since the first prototype was announced in 2008,[1] memristors[2] have attracted broad interests over the past several years due to their potentials for non-volatile memory,[3,4] artificial neural networks,[5,6] chaotic circuits,[7,8] logic operation,[9] signal processing,[10] and so on. The resistance of a memristor can change under the action of electric field or current, and this change is non-volatile and reversible. A broad category of materials and structures have been included in memristors, and a typical memristor is constructed from either capacitor-like or planar metal-oxide-metal (MIM) structures.[11,12] While most of current research on MIM memristors focus on their electronic behaviors, their optical properties, especially the electroluminescence (EL) related to their resistance states, i.e. high resistance state (HRS) and low resistance state (LRS), were rarely investigated.[13–15] Here we report the first realization of the electroluminescence and the resistive switching simultaneously in the same planar nanogapped memristor device. These devices have planar MIM structures using nanogapped graphene as electrodes and SiO_2 as dielectric layer. The light emission ranging at 400–1100 nm that can be tuned by the device's resistance states was found, and prototype of light-emitting sources for displays and pulsed signaling were demonstrated. An electron-hole recombination EL mechanism for Si nanocrystals (NCs) in these devices was proposed and evidenced by our spectroscopic and structural characterizations. The combination of memristor and EL may bring new functionalities for this type of devices, e.g. potential use of these optical signals to detect the devices' resistance states. Our results may be very important for future nanoelectronic and optoelectronic applications, such as a very promising light source, light-pulse generator, optical switching, optical communication, even optical amplifiers, silicon lasers and photovoltaics.

C. He, P. Chen, J. Zhao, M. Cheng, W. Yang,
G. Xie, D. Wang, D. Liu, R. Yang, D. Shi, G. Zhang
Nanoscale Physics and devices Laboratory
Beijing National Laboratory for Condensed
Matter Physics and Institute of Physics
Chinese Academy of Sciences, Beijing, 100190, China
E-mail: gyzhang@aphy.iphy.ac.cn
J. Li, Z. Li
Laboratory of Optical Physics
Beijing National Laboratory for Condensed Matter Physics
and Institute of Physics
Chinese Academy of Sciences
Beijing, 100190, China
X. Wu, K. Yin, L. Sun
SEU-FEI Nano-Pico Center
Key Laboratory of MEMS of Ministry of Education
School of Electrical Science and Engineering
Southeast University
210096, Nanjing, China

DOI: 10.1002/adma.201302447

Figure 1a shows the image of the as-made two-terminal memristor devices array. Atomic force microscopy (AFM) image of an individual device with width of 5 μm and length of 600 nm after forming process reveals a planar memristor structure with nanogapped graphene film as electrodes and SiO_2 as conduction channel. Polycrystalline graphene film was directly grown on SiO_2 substrates using a remote plasma assisted chemical vapor deposition techniques. Refer to our previous paper for the device fabrication process.[16] Resistances of this type of devices can be tuned from LRS ("ON") to HRS ("OFF") via set and reset voltages. Note that all electrical operation and measurements were carried out in vacuum of $<2 \times 10^{-4}$ Torr at room temperature, and the optical measurements were performed in a dark room. The dc sweep *I-V* properties and constant bias were characterized by an Agilent 4156C semiconductor parameter analyzer. Figure 1b shows a typical *I-V* switching characteristic of a memristor device under dc voltage sweep. In the set process, the current jumps abruptly at V_{set} = ~3 V to ON state from OFF state. The device recovers to OFF state at V_{reset} = ~7 V when sweeping voltage from 0 to 11 V in the reset process. The ON/OFF ratio is ~10^5 as marked by the vertical dashed line. During the electrical operation for a memristor device from LRS to HRS, strong light emission accompanying with the *I-V* switching process was observed, which was even visible by naked eyes. Figure 1c illustrates the light emission at different resistance states as well as bias voltages (V_b) for the memristor devices, imaged by a charge coupled device (CCD) camera connected to a long focal distance microscope. We can see that the EL intensity increased with V_b, reached maximum at 5–6 V, and gradually weakened at $V_b > 6$ V.

The EL spectra were collected by spectrometer connected to a microscope through an optical fiber, as illustrated in **Figure 2**a. The EL spectra of the above-mentioned device at V_b = 5 V (LRS) and V_b = 11V (HRS) collected at an integration time of 5 s are shown in Figure 2b. We can see that the light emission covers the entire visible light and near-infrared range of 400–1100 nm and shows a broadened peak centered at 770 nm and 550 nm for LRS and HRS, respectively. The dynamic characteristic of the EL was measured by monochromator targeting on the wavelength of 750 nm. The amplitude of LRS EL peak is an order of magnitude higher than that for HRS, indicating a potential

© 2013 WILEY-VCH Verlag GmbH & Co. KGaA, Weinheim

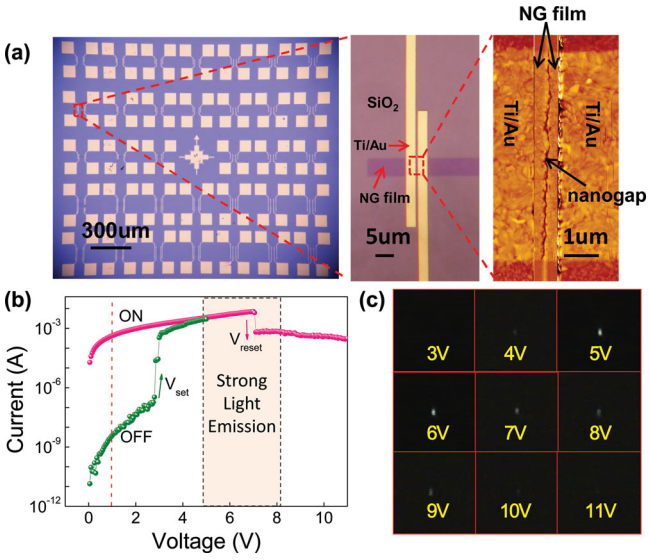

Figure 1. (a) Optical image of the memristor array (left) and an individual device (middle). Zoom-in AFM image of this device (right) shows a planar graphene/SiO_2 nanogap structure, revealing a broken gap region marked by a black arrow in the middle of graphene electrodes clearly. (b) Typical *I-V* switching characteristics of a device with graphene width of 5 µm and length of 600 nm. The dashed rectangle marked region is strong light emitting region. (c) The CCD images of the EL phenomenon of the memristor device with different driven voltages.

use of these optical signals for detection of the devices' resistance states. Besides, the wavelength of this EL peak is tunable by applied bias V_b. 500 s time-trace of the device at LRS with applied bias of 7.5 V (Figure 2c) reveals a stable light emission over a long duration. In addition, the EL behaviors were also observed in the memristor devices using quartz glass (figure S1) instead of SiO_2(300 nm)/Si(500 µm) as dielectric substrates, showing the potential for developing low-cost full-transparent optoelectronic devices.

EL devices have been broadly used as various light sources such as lamps or information displays.[17,18] Here we illustrate such applications using the present planar graphene/SiO_2 nanogap memristor devices. **Figure 3**a shows the optical image of the memristors with various widths of 2 µm, 5 µm, 10 µm, and 25 µm. The SEM images of the light-emitting devices were indicated in (a-d) of Figure S2. The EL images of them were captured at V_b = 7.5 V. We can see that the light-emission source gradually transforms from a point source into a line source as the width of the device increases from 2 µm to 25 µm (Figure 3b). Figures 3c and 3d show the optical and corresponding EL images of a 3 × 3 memristors array. Different emission patterns were demonstrated by tuning the individual devices' resistance states. We also show an EL display of a Latin letter "N" after a violent electrical breakdown process (see supplementary movie).

As shown above, EL of a memristor device is strong and directly related to its resistance states; thus we could use it for generation of light pulses by tuning its resistance states, e.g., set/reset voltages. **Figure 4** shows the time-resolved EL trace measured at peak position of ~770 nm with driving voltage pulse of 7.5V/200 ns. The measured rise and decay time for

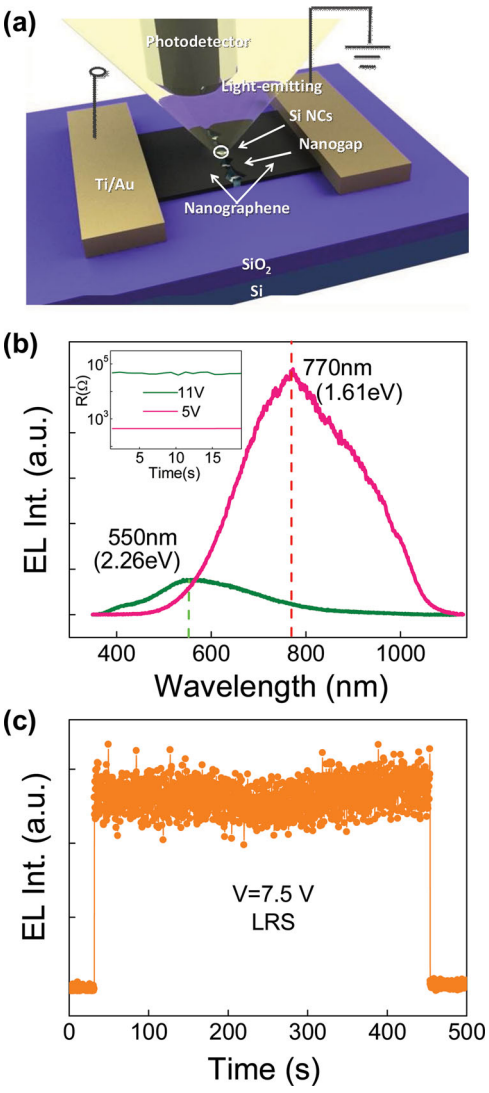

Figure 2. Static EL characteristics of the memristor. (a) Schematic diagram of electrical and optical measurements. (b) The EL spectra of the memristor with LRS and HRS. The EL peaks of LRS and HRS are at around 770 nm and 550 nm, respectively. The inset is the low and high resistance state when applying constant bias of 5 V and 11 V, respectively. (c) The EL Intensity versus time of the memristor at LRS applied bias of 7.5 V.

the generated light pulse is τ_{rise} = 0.7 µs and τ_{decay} = 17.7 µs (see below for more details). Thus, this simple and low-cost structure can be used to generate microsecond light pulses. In Figure 4b, we demonstrate a series of light pulses (bottom panel) generated by applying electrical pulses (top panel) with width of 200 ns, amplitude of 7.5 V, and frequency of 5 kHz. The optical signal can be programmed by applied electrical signals. This programmable and tunable generation of optical pulses might be useful for future nano-optoelectronic applications.

In our previous work, we proposed that Si NCs embedded in the SiO_2 matrix of the gap region formed by the forming process are accounted for the resistance switching in the planar graphene/SiO_2 nanogap memristor.[16] We believe that these

© 2013 WILEY-VCH Verlag GmbH & Co. KGaA, Weinheim
Adv. Mater. 2013,
DOI: 10.1002/adma.201302447

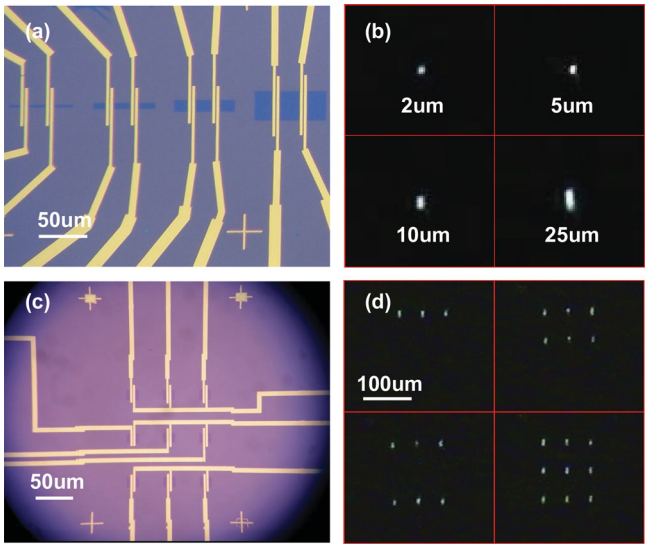

Figure 3. Planar graphene/SiO_2 nanogap structures in application for lighting and displays. (a) The optical microscope image of the memristors with various widths of 2, 5, 10, and 25 µm. (b) The CCD images of the EL behavior of the memristors with different widths at bias voltage of 7.5 V. (c) and (d) are the optical image and CCD image of the EL phenomenon of an array of 3 × 3 devices.

Si NCs also play a very important role in the observed EL process in these planar memristor devices, which is ascribed to the recombination of electrons and holes injected into the Si NCs. Such conclusions are based on two facts: 1) The energy distributions of the EL are closely related to the resistance states of a memristor; 2) Very short τ_{rise} and τ_{decay} further confirm that the EL is light emitting process due to recombination of electron-hole pairs rather than a radiation induced by heat dissipation.

In order to experimentally confirm the existence of Si NCs in these planar memristor devices, we carried out high resolution transmission electron microscopy (HRTEM) imaging of the devices. The devices were pre-switched into ON or OFF state and focused ion beam (FIB) In-situ lift-out techniques were used for sample preparation. **Figure 5**a shows the scanning electron microscope (SEM) image of a typical device (top view) with nanogap region marked by the dashed white line. Then the nanogap regions of both LRS and HRS were cut out by in-situ lift-out FIB technique. Figure 5b shows a cross section SEM image of this device after FIB-cut. Two example HRTEM images of such devices at OFF state and ON state are shown in Figure 5c and 5d, respectively. HRTEM observations reveal three important features: 1) The existence of NCs embedded in the amorphous SiO_x is always present at both ON and OFF states. The marked two lattice spacing of 0.31 nm and 0.18 nm correspond to the Si(111) plane and Si(220) plane, respectively.[19,20] 2) The sizes of the OFF-state Si-NCs are usually smaller than 3 nm, while they are usually larger than 5 nm at On -state. 3) The OFF-state Si-NCs are isolated with an average gap of >5 nm; while ON-state Si-NCs tend to be closely packed with much smaller gaps. These features support our above understanding of the resistive switching phenomena in our memristor devices. We also conclude that the different sizes of Si NCs at OFF state and ON state are the causes for different peak wavelength light emitting at OFF and ON states.

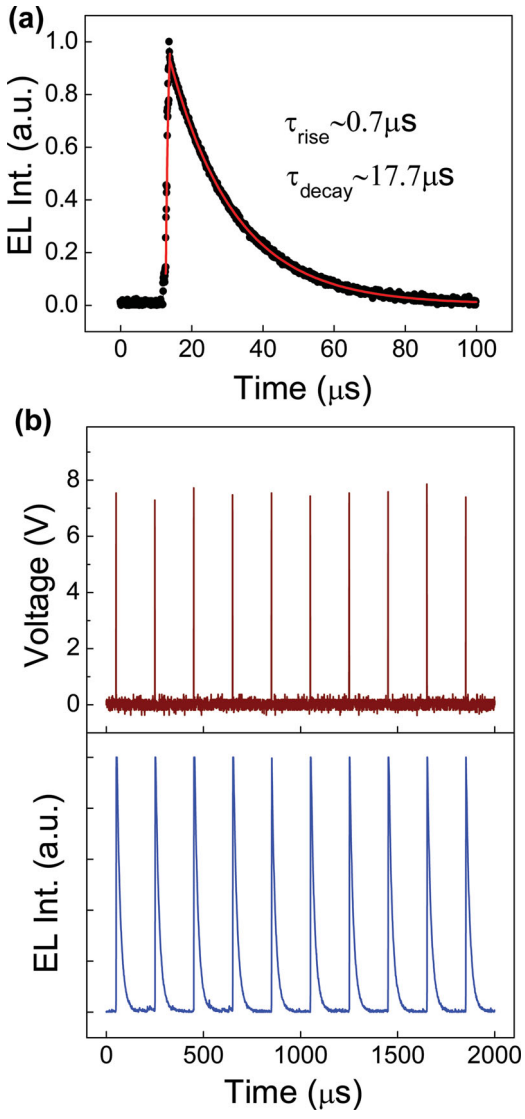

Figure 4. Time-resolved EL intensities measured at the EL peak value ~770 nm with voltage pulse of 7.5 V and 200 ns. (a) The decay profile of EL and the decay time τ_{decay} ~ 17.7 µs extracted from fitting an exponential line shape to EL decay curve, and the rise time of EL, τ_{rise} ~ 0.7 µs. (b) A series of light pulses (bottom panel) generated by applying electrical pulses (top panel) with width of 200 ns, amplitude of 8 V and frequency of 5 kHz.

The study of luminescence of Si NCs dispersed in a SiO_2 matrix is a very active research field recently, because of the interesting fundamental physical properties and of promising applications in advanced electronic devices and optoelectronic devices, which open new opportunities of Si-based optoelectronics.[21–25] EL of Si NCs is commonly described by the equation: $I(t) = I_0\exp[-(t/\tau)^{\beta}]$.[26–30] Here I_0 is the time-dependent EL intensity at $t = t_0$; τ is the effective recombination lifetime (decay time); β is the dispersion factor between 0 and 1, and $\beta = 1$ represents a system with isolated Si NCs. In Figure 4a, $\beta = 0.96$ and $\tau = 17.7$ µs can be extracted via fitting the EL decay curve with the EL intensity equation. The extracted β close to 1

© 2013 WILEY-VCH Verlag GmbH & Co. KGaA, Weinheim

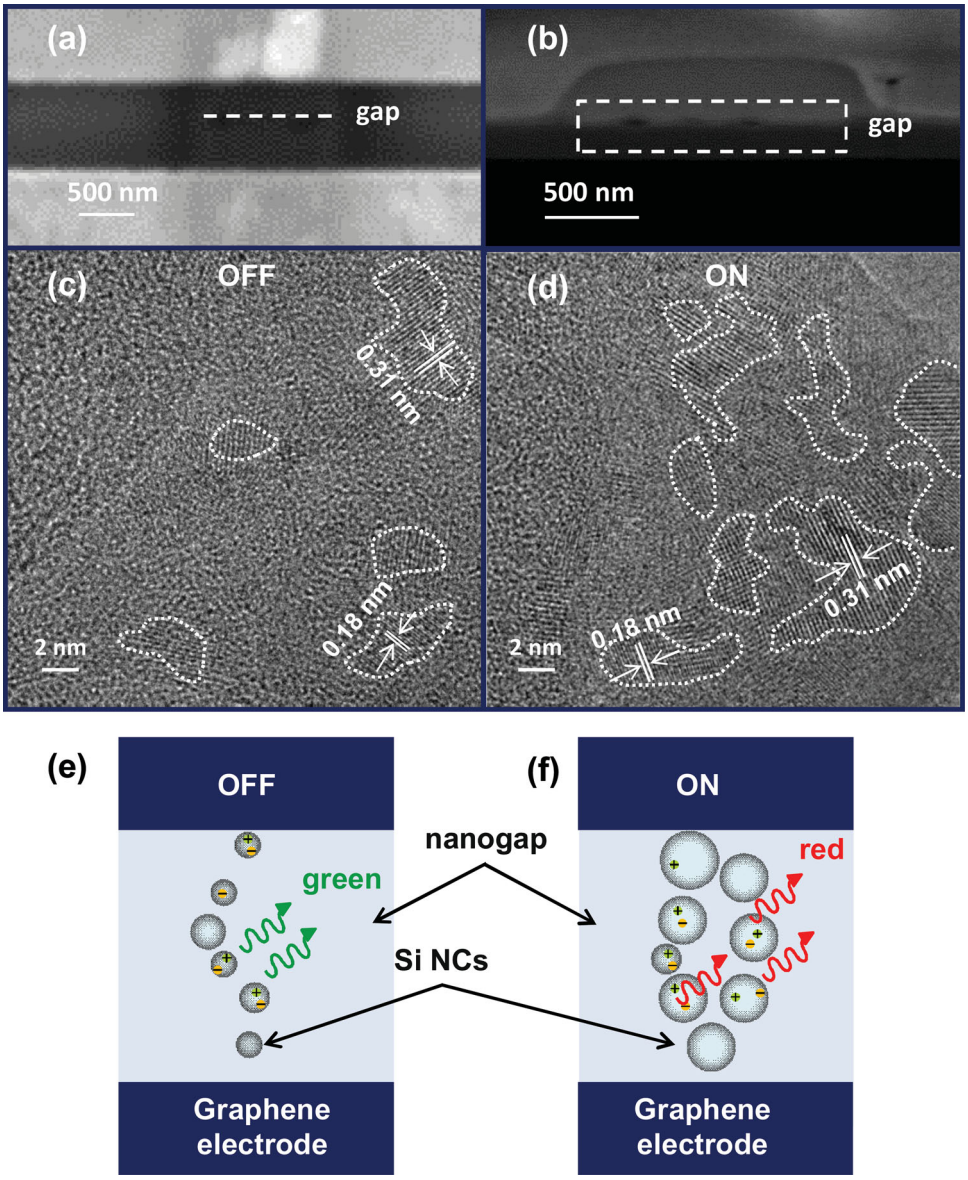

Figure 5. The EL mechanism in the planar graphene/SiO_2 nanogap structure memristor. Recombination of the electrons and holes injected into the Si NCs with in the nanogap results in the emission of light. HRTEM imaging of the devices were carried out to experimentally confirm the existence of the Si NCs in these planar memristor devices (a–d). (a) The SEM image of the switching planar graphene/SiO_2 nanogap structure (top view). The dashed white line indicates the confined nanogap site, which location is the FIB-cut along with. (b) The side view SEM image of cross section corresponding to the dashed white line in (a). HRTEM images of the nanogap region as indicated by white dashed rectangle in (b) with the devices at OFF state (c) and ON state (d). Nanocrystalline structures are delineated by white dashed lines. The lattice spacing of the NCs is either at 0.31 nm or at 0.18 nm, corresponding to that in a Si(111) plane and a Si(220) plane. The sizes of Si NCs of OFF state are usually smaller than 3 nm, whereas that of ON state are always greater than 5 nm. (e–f) are schematic diagram of the EL mechanism. The wavelength of the emission light is determined by the bandgap of the Si NCs, which depend on the size of the Si NCs cluster. The Si NCs in the nanogap of OFF state were shown in (e), the size of which are mostly distributed in 2 ~ 3 nm deduced from the green EL spectra. (f) indicates the Si NCs in the nanogap of ON state, the size of which are mostly distributed in 4 ~ 5 nm inferred from the red emission.

reveals that such a system behaves more like isolated crystals. This may be explained by that exciton diffusion in the system is very much suppressed due to the fast nonradiative recombination. The rise time constant τ_{rise} of EL is ~0.7 μs. The rise time and decay time exhibited no obvious dependence on the driving pulse width and the detected wavelength (shown in Figure S3). We measured many devices and found that the rise time constant is always <1μs, the decay time around ~18.0 μs, and the value of β is around 0.96–0.98.

Several models have been proposed to explain the luminescence in Si NCs, including quantum confinement,[31,32] surface states,[33] and defects in the oxide.[34] For simplicity, here we only consider quantum confinement effects. Resemble single exponential EL decay curves reveal that surface states

© 2013 WILEY-VCH Verlag GmbH & Co. KGaA, Weinheim

DOI: 10.1002/adma.201302447

and defects have a negligible impact on the radiative recombination mechanism. Recombination of the electrons and holes injected into the isolated NCs results in the emission of light. Figure 5e–f indicates the schematic diagram of the EL mechanism in a planar graphene/SiO_2 nanogap memristor. The wavelength of the emission light depended on the bandgap of the NCs, which is determined by the size of the Si NCs. The broad EL spectrum (across the range from 400 to 1100 nm) reflects the size distribution of Si NCs. The green EL spectra of HRS state and the red emission of LRS state illustrate the size dependence of Si NCs formed at LRS and HRS. Following the quantum confinement model, the peak EL energy is equal to the free exciton band gap. This can be used to deduce the average size of the Si NCs in the nanogap of HRS and LRS states, which are most distributed around in 2 ~ 3 nm and 4 ~ 5 nm,[35–38] respectively, in consistence with our TEM results.

In conclusion, EL behaviors in planar graphene/SiO_2 nanogap memristors were observed. The EL spectra cover the wavelength range from 400 to 1100 nm. The EL behaviors are attributed to recombination of the electrons and holes injected into the NCs located within the nanogap that is subject to quantum confinement effect. The EL peaks can be tuned between 550 nm and 770 nm reliably and controllably via setting the device to different resistance states, i.e., HRS and LRS, thus altering the size of the Si NCs in the device. The rise and decay time constant of the EL process were measured with τ_{rise} = 0.7 μs and τ_{decay} = 17.7 μs, respectively. The connection between device's resistance states and EL can be used to identify each other. Our results point to the possibility of using this simple structure for creating light-emitting structures for optical communications photonic integrated circuits across the spectral region 400–1100 nm. In addition, the fabrication process of these light-emitting memristor is simple, low-cost, scalable and fully compatible with silicon-based technologies. The simple nanogap structure may be very important for future nanoelectronic and optoelectronic applications.

Experimental Section

Imaging of the graphene/SiO_2 nanogap structures: An atomic force microscope (Multi-Mode IIId, Veeco Instruments Inc.) was used for imaging the nanogap in the middle of the NG film. The SEM images were obtained by the SEM mode of Raith e-line e-beam lithography system. For the HRTEM analysis, the TEM sample was prepared by focused ion beam (FIB) using a gallium beam in a dual beam Helios system from FEI. The device was switched ON or OFF state by dc voltage sweeping before FIB-cut. Then the nanogap regions of both LRS and HRS were cut out by in-situ lift-out FIB technique. Low-kV cleaning process was used to remove the surface amorphous layer. After TEM sample preparation, HRTEM was carried out using an image aberration-corrected TEM (FEI Titan 80–300) with an acceleration voltage of 30 kV.

Measurements of electrical characteristics of the devices: The dc sweep *I-V* properties and constant bias were characterized by an Agilent 4156C semiconductor parameter analyzer in vacuum of $<2 \times 10^{-4}$ Torr at room temperature. Agilent 33250A pulse generator was used to measure the EL decay time and to generate the light pulse. The semiconductor parameter analyzer and the pulse generator were connected the vacuum chamber by using triax cables. The device was load onto a chip carrier inside the measurement vacuum chamber with the Ti/Au electrode pads attached to the chip carrier through wire-bonding, which were connected to the atmosphere via a feed-through.

Characterization of the EL in the graphene/SiO_2 nanogap structure memristors: In our optical measurements, the light from the memristor was collected by a long focal distance microscope objective, imaged by a charge coupled device (CCD, HITACHI, KP-D20) camera connected to the microscope. The EL spectra were measured by using a spectrometer (Ocean Optics, QE6500) connected to the microscope through an optical fiber. A monochromator (Zolix, Omni-λ300) equipped with a fast photomultiplier tube (Hamamatsu, H7422P-50) and an oscilloscope (Agilent, DSOX3054A) were used to measure and record the dynamic characteristics of the EL behavior.

Supporting Information

Supporting Information is available from the Wiley Online Library or from the author.

Acknowledgment

G.Z. acknowledges financial support from the National Basic Research Program of China (973 Program) under the grant No. 2013CB934500 and the National Science Foundation of China (NSFC) under the grant Nos. 91223204, 11204358, and 11174333. L.S. acknowledges financial support from the 973 programs (2011CB707601, 2009CB623702) and Chinese postdoctoral funding (No. 2012M520053) and Jiangsu Province Funds for Distinguished Young Scientists (No. BK2012024).

Received: May 29, 2013
Revised: June 24, 2013
Published online:

[1] D. B. Strukov, G. S. Snider, D. R. Stewart, R. S. Williams, *Nature* **2008**, *453*, 80.
[2] L. O. Chua, *IEEE Transactions on Circuit Theory* **1971**, *CT18*, 507.
[3] J. J. Yang, M. D. Pickett, X. M. Li, D. A. A. Ohlberg, D. R. Stewart, R. S. Williams, *Nat. Nanotechnol.* **2008**, *3*, 429.
[4] H. Yenpo, G. M. Huang, L. Peng, *Proc. 2009 IEEE/ACM ICCAD* **2009**, 485.
[5] S. H. Jo, T. Chang, I. Ebong, B. B. Bhadviya, P. Mazumder, W. Lu, *Nano Lett.* **2010**, *10*, 1297.
[6] M. K. Hota, M. K. Bera, B. Kundu, S. C. Kundu, C. K. Maiti, *Adv. Funct. Mater.* **2012**, *22*, 4493.
[7] B. Muthuswamy, P. P. Kokate, *Memristor-Based Chaotic Circuits. IETE Tech. Rev.* **2009**, *26*, 417.
[8] W. H. Sun, C. F. Li, J. B. Yu, *Ieee, A Memristor Based Chaotic Oscillator*, Ieee: New York, **2009**, 955.
[9] J. Borghetti, G. S. Snider, P. J. Kuekes, J. J. Yang, D. R. Stewart, R. S. Williams, *Nature* **2010**, *464*, 873.
[10] Y. Yilmaz, P. Mazumder, *2012 IEEE 12th Int. Conf. Nanotechnol.* **2012**, 1–4.
[11] R. Waser, M. Aono, *Nat. Mater.* **2007**, *6*, 833.
[12] Y. B. L. Y. B. Li, A. Sinitskii, J. M. Tour, *Nat. Mater.* **2008**, *7*, 966.
[13] T. W. Hickmott, *J. Vacuum Sci. Technol.* **1969**, *6*, 828.
[14] S. F. Alvarado, F. La Mattina, J. G. Bednorz, *Appl. Phys. a - Mater.* **2007**, *89*, 85.
[15] A. A. Zakhidov, B. Jung, J. D. Slinker, H. D. Abruna, G. G. Malliaras, *Org. Electron* **2010**, *11*, 150.
[16] C. L. He, Z. W. Shi, L. C. Zhang, W. Yang, R. Yang, D. X. Shi, G. Y. Zhang, *ACS Nano* **2012**, *6*, 4214.
[17] R. H. Friend, R. W. Gymer, A. B. Holmes, J. H. Burroughes, R. N. Marks, C. Taliani, D. D. C. Bradley, D. A. Dos Santos,

© 2013 WILEY-VCH Verlag GmbH & Co. KGaA, Weinheim

J. L. Bredas, M. Logdlund, W. R. Salaneck, *Nature* **1999**, *397*, 121.
[18] R. H. Kim, M. H. Bae, D. G. Kim, H. Y. Cheng, B. H. Kim, D. H. Kim, M. Li, J. Wu, F. Du, H. S. Kim, S. Kim, D. Estrada, S. W. Hong, Y. G. Huang, E. Pop, J. A. Rogers, *Nano Lett.* **2011**, *11*, 3881.
[19] Y. Q. Wang, T. Li, W. S. Liang, X. F. Duan, G. G. Ross, *Nanotechnology* **2009**, *20*, 315704.
[20] J. Yao, Z. Z. Sun, L. Zhong, D. Natelson, J. M. Tour, *Nano Lett.* **2010**, *10*, 4105.
[21] L. Pavesi, L. Dal Negro, C. Mazzoleni, G. Franzo, F. Priolo, *Nature* **2000**, *408*, 440.
[22] J. Valenta, N. Lalic, J. Linnros, *Appl. Phys. Lett.* **2004**, *84*, 1459.
[23] R. J. Walters, G. I. Bourianoff, H. A. Atwater, *Nat. Mater.* **2005**, *4*, 143.
[24] P. M. Fauchet, *Mater. Today* **2005**, *8*, 26.
[25] V. Beyer, B. Schmidt, K. H. Heinig, K. H. Stegemann, *Appl. Phys. Lett.* **2009**, *95*, 193501.
[26] Y. Kanemitsu, *Phys. Rev. B* **1994**, *49*, 16845.
[27] P. J. Ventura, M. C. Docarmo, K. P. Odonnell, *J. Appl. Phys.* **1995**, *77*, 323.
[28] J. Linnros, N. Lalic, A. Galeckas, V. Grivickas, *J. Appl. Phys.* **1999**, *86*, 6128.
[29] A. Irrera, D. Pacifici, M. Miritello, G. Franzo, F. Priolo, F. Iacona, D. Sanfilippo, G. Di Stefano, P. G. Fallica, *Appl. Phys. Lett.* **2002**, *81*, 1866.
[30] A. Anopchenko, A. Marconi, E. Moser, S. Prezioso, M. Wang, L. Pavesi, G. Pucker, P. Bellutti, *J. Appl. Phys. Lett.* **2009**, *106*, 033104.
[31] P. K. Basu, *Proceeding of the Tenth International Workshop on the Physics of Semiconductor Devices*, Vols *I and Ii*, V. Kumar, S. K. Agarwal, Eds. Spie-Int Soc Optical Engineering: Bellingham, **2000**, *3975*, 937.
[32] N. M. Park, T. S. Kim, S. J. Park, *Appl. Phys. Lett.* **2001**, *78*, 2575.
[33] F. Koch, V. Petrovakoch, T. Muschik, *J. Lumines.* **1993**, *57*, 271.
[34] S. M. Prokes, *Appl. Phys. Lett.* **1993**, *62*, 3244.
[35] J. P. Proot, C. Delerue, G. Allan, *Appl. Phys. Lett.* **1992**, *61*, 1948.
[36] M. V. Wolkin, J. Jorne, P. M. Fauchet, G. Allan, C. Delerue, *Phys. Rev. Lett.* **1999**, *82*, 197.
[37] J. Heitmann, F. Muller, M. Zacharias, U. Gosele, *Adv. Mater.* **2005**, *17*, 795.
[38] P. D. Nguyen, D. M. Kepaptsoglou, Q. M. Ramasse, A. Olsen, *Phys. Rev. B* **2012**, *85*, 085315.

© 2013 WILEY-VCH Verlag GmbH & Co. KGaA, Weinheim
Adv. Mater. **2013**,
DOI: 10.1002/adma.201302447